Determination of hydraulic conductivity of a suspension

Marketa Petrova, Jiri Mls [*]

Charles University in Prague, Faculty of Science, Albertov 6, 128 43 Praha 2, Czech Republic.
[*] Corresponding author. E-mail: mls@natur.cuni.cz

Abstract: The process of sedimentation and subsequent gravity compression of kaolin and water suspensions was investigated experimentally. 45 batch tests were carried out and the time dependence of the height of the suspension column was measured. The one-dimensional equations of Darcian mechanics of two-phase porous media are applied to formulate the studied process mathematically. A very natural assumption makes it possible to find a solution of the forward problem for a starting period of the process. Analysis of the theoretical function and the experimental data gives hydraulic conductivity as a function of the suspension concentration. The obtained results are presented and discussed.

Keywords: Hydraulic conductivity; Kaolin; Suspension; Gravity thickening.

INTRODUCTION

Various industrial technologies require to study the process of suspension sedimentation and dewatering. According to its energetic efficiency, the gravitational thickening is one of the mostly utilized methods of lowering volume of suspensions and increasing the concentration of their solid phase. There are two kinds of standard laboratory tests, the batch tests and the continuous tests, which are utilized when examining the thickening process or when collecting data required for its mathematical modelling.

The presented research was aimed at carrying out a set of experiments with a well defined suspension of water and kaolin and to develop a convenient method of getting hydraulic conductivity of the suspension as a function of its concentration.

Numerous authors have presented contributions to experimental or theoretical study of suspension thickening processes. To cite the classical ones, we can start with (Coe and Clevenger, 1916) and continue with well known paper by Kynch (1952) whose results were often adopted in later research. In our research, the degree of the suspension coagulation and gel point position were important and hence, we made use of the paper by Usher and Scales (2005) and particularly of results presented by Nasser and James (2007), who utilized a modified version of the model originally suggested by Landman et al. (1988). In this way, Nasser and James (2007) were able to consider hindered settling and the effect of the gel point. It should be mentioned that there are studies of suspensions without coagulation and with negligible thickening, e.g. Vlasák et al. (2012).

As the process we study is time-dependent, we make use of the Darcian-mechanics equations published by Mls (1999). The efficiency of this theory has already been proved particularly when solving the problem to determine the height of the suspension column and the position of the gel point under conditions of a continuous dewatering process (Mls, 2005). Though the equations contain Darcy's law, they are not parabolic, for discussion see Mls and Herrmann (2011). To formulate general one-dimensional process, the theory requires two parameters that are functions of the suspension concentration. The paper is aimed at presenting determination of one of them.

THE APPLIED THEORY

According to Mls (1999), the general flow of both the solid phase and the liquid phase in one dimension is governed by following equations

$$\frac{\partial n}{\partial t}(x,t) + \frac{\partial w}{\partial x}(x,t) = 0, \tag{1}$$

$$\frac{\partial n}{\partial t}(x,t) - \frac{\partial v}{\partial x}(x,t) = 0, \tag{2}$$

$$\frac{\partial w}{\partial t}(x,t) + gn(x,t) + \frac{n(x,t)}{\rho_w}\frac{\partial p}{\partial x}(x,t) + \frac{gn(x,t)}{K(x,t)}u(x,t) = 0, \tag{3}$$

$$\frac{\partial v}{\partial t}(x,t) + g(1-n(x,t)) - \frac{1}{\rho_s}\frac{\partial \tau}{\partial x}(x,t) + \\ + \frac{1-n(x,t)}{\rho_s}\frac{\partial p}{\partial x}(x,t) - \frac{g\rho_w n(x,t)}{\rho_s K(x,t)}u(x,t) = 0, \tag{4}$$

where n is porosity of the suspension, x is the space coordinate oriented vertically upwards, t is time, w and v are the liquid-phase and the solid-phase volumetric flux densities, respectively, g is gravity acceleration, ρ_w and ρ_s are the liquid-phase and the solid phase densities, respectively, ρ is the liquid-phase pressure, K is hydraulic conductivity of the suspension, τ is the solid-phase stress and u is the relative liquid-phase volumetric flux density satisfying relation

$$u = w - \frac{n}{1-n}v. \tag{5}$$

Eqs (1) and (2) are continuity equations of the liquid phase and the solid phase, and Eqs (3) and (4) are equations of motion of the liquid phase and the solid phase. The steady state form of Eq. (3) is Darcy's law.

Let the considered suspension be placed in a vessel with an impervious bottom, which is the case we will study below, and let the initial height of the suspension column be L. The considered domain is then

$$\Omega = \left\{ x; x \in (0, L) \right\}, \tag{6}$$

and the boundary conditions imposed at $x = 0$ on w and v are

$$w(0,t) = 0 \quad \text{and} \quad v(0,t) = 0 \quad \text{for} \quad t > 0. \tag{7}$$

From Eqs (1) and (2) we get a simple differential equation

$$\frac{\partial (w+v)}{\partial x}(x,t) = 0,$$

which can be easily solved. All its solutions are

$$w(x,t) + v(x,t) = f(t),$$

where f is any differentiable function. To satisfy conditions (7), f has to be zero. Hence

$$w(x,t) = -v(x,t) \quad \text{for} \quad (x,t) \in [0,L] \times [0,\infty), \tag{8}$$

Making use of Eqs (5) and (8) and excluding the derivative $\dfrac{\partial p}{\partial x}$ from Eqs (3) and (4), the set of governing equations can be reduced to the continuity Eq. (1)

$$\frac{\partial n}{\partial t}(x,t) + \frac{\partial w}{\partial x}(x,t) = 0,$$

and the equation of motion

$$\frac{\partial w}{\partial t} + \frac{n}{\rho_w + n(\rho_s - \rho_w)}\frac{\partial \tau}{\partial x} = \frac{g(\rho_s - \rho_w)n(1-n)}{\rho_w + n(\rho_s - \rho_w)} -$$
$$- \frac{g\rho_w n}{(1-n)K(\rho_w + n(\rho_s - \rho_w))}w. \tag{9}$$

These equations contain two unknown functions, n and w, all the other functions are supposed to be given parameters. Particularly the hydraulic conductivity must be known, when solving problems with Eqs (1) and (9). In this paper, we focus on the problem of determining hydraulic conductivity of kaolin suspensions. The suspension concentration defined as mass of the solid phase contained in unit volume of the suspension, i.e.

$$c = \rho_s (1-n), \tag{10}$$

is generally used to describe the state of a suspension. In order to respect this, we replace porosity n by concentration c in the following text.

We will suppose that under conditions of monotonous processes, hydraulic conductivity K and solid-phase stress τ are functions of the suspension's concentration. The notion of the monotonous process was introduced by Mls (1995) in order to exclude a possible effect of hysteresis: a process in a suspension is monotonous when it satisfies the condition

$$\frac{\partial c}{\partial t}(m_1,t_1)\frac{\partial c}{\partial t}(m_2,t_2) \geq 0, \tag{11}$$

for any couple of values m_1 and m_2 of a material coordinate and for any couple of instants t_1 and t_2.

THE MATERIAL OF THE SUSPENSION

The experimental research was carried out with suspensions of water and kaolin. Among the available materials, the Sedlec kaolin Zettlitz Ia was chosen as it is a well defined material making it possible to repeat the experiments at any time later. Moreover, it is also suitable because of its well-balanced granulometric curve, see Fig. 1 and Table 1. The particle size distribution was measured with the SediGraph ET 5000, manufactured by the Micromeritics. The sedigraph measures particle mass directly via X-ray absoption and determines the equivalent spherical diameter of particles from the rate at which particles fall under gravity through a liquid having known properties. The data presented in Fig. 1 and Table 1 are affected by the accuracy of the described method of measurement. The applied water was deionized before it was used in suspensions.

Kaolinite is a layered silicate mineral with one tetrahedral sheet of SiO_4 linked through oxygen atoms to one octahedral sheet of Al_2O_3. Within the kaolinite structure, there are isomorphous substitutions possible: Silicate (4+) can be surrogated by Al(3+) or by Fe(3+). If so, kaolinite particle carries negative charge on its surface, van Olphen (1963). Table 2 shows the composition of the applied kaolin.
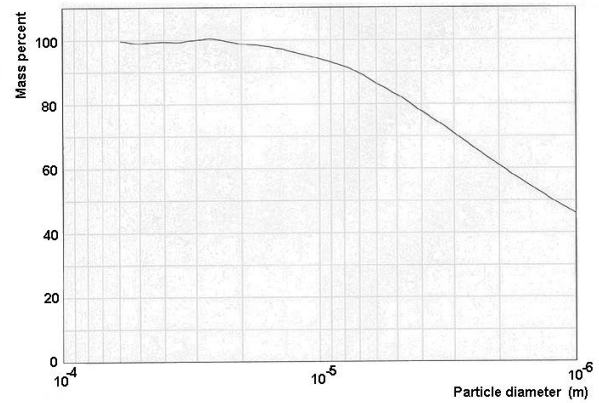

Fig. 1. Kaolin Zettlitz Ia – granulometric curve.

Table 1. Kaolin Zettlitz Ia – granulometric distribution.

D (μm)	50	40	30	25	20	15	10	8
Mass (%)	99.0	99.4	100.0	100.2	98.7	97.5	94.1	91.7
D (μm)	7	6	4	3	2	1.5	1	
Mass (%)	89.6	86.4	77.7	70.9	60.9	54.4	45.9	

If the particles are mechanically damaged, the linkage of Al-O-Al or Si-O-Si is disconnected. In water environment, groups of Al-OH or Si-OH arise. Under acidic conditions, which was our case as we worked with pH between 5.8 and 6.2, Al-OH groups loose hydroxide ion and Si-OH groups stay unchanged. Now, surfaces carry a negative charge whilst the charge of edges is positive and the edges and faces attract each other giving rise to a face – edge coagulation and the resulting structure is known as the "card-house" coagulum (Šatava, 1973).

Kaolin Zettlitz Ia is not a raw material. In the course of fabrication it is enriched by calcium (II) and sodium cations which stimulate the coagulation. On the other hand, the degree of coagulation is too small to create a clearly visible interface between the suspension and the overlying layer of water. As it

was necessary to measure the position of this interface with a good accuracy and for a relatively wide range of suspension concentrations, a precise rate of coagulation was defined. At any applied suspension concentration, the coagulation was achieved by adding Calcium(II) chloride at 0.4 percent of the solid-phase mass.

Table 2. Composition of the Kaolin Zettlitz Ia.

SiO$_2$	Al$_2$O$_3$	Fe$_2$O$_3$	TiO$_2$	CaO	MgO	K$_2$O	Na$_2$O	Loss on ignition
47.28	35.78	0.97	0.26	0.29	0.23	1.05	0.03	14.02
Kaolinite				91%				
Quartz				2%				
Mica				7%				

Vertical cylinders with impervious bottom were used to carry out the settling experiments. The height of the cylinders was 2000 mm and, in most cases, their inner diameter was 104 mm. Several cylinders having inner diameters 94 and 114 mm were also used in order to check whether the results were affected by the cross-section surface and perimeter.

THE LABORATORY MEASUREMENTS

A set of 45 batch tests has been carried out in the laboratory of Department of Hydrogeology at Charles University. The applied suspensions were mixtures of the above described kaolin and water in the precisely defined state of coagulation. A homogeneous mixture was prepared in a tank and was poured into the vessel used for the measurements immediately that after. According to this procedure, we supposed that each test started from homogeneous state of the suspension column. Hence the initial conditions of an experiment are

$$c(x,0)=c_0 \text{ and } w(x,0)=0 \quad \text{for } x \in (0,L), \tag{12}$$

where L is the initial height and c_0 is the initial concentration of the suspension column at the experiment. A visible interface develops in the suspension during the sedimentation process.

The interface separates the zone of suspension from the overlying layer of water and moves downwards starting at time $t = 0$ from the level $x = L$. We will denote with $Z(t)$ its height above the bottom at time t. The thickening of the suspension begins at the impervious bottom where the particles of the solid phase are stopped. Consequently, another interface starts its motion from the bottom upwards, separating the layer of suspension of the initial concentration c_0 from the zone of thickening, see Fig. 2. As the upper interface is clearly visible, it was possible to measure the time dependence of the height of the suspension column. In this way, 45 batch tests were carried out each one for particular initial values of concentration c_0 and height L.

The data obtained during a test are of the form

$$\left\{ (t_i, z_i) \right\}_{i=0}^{N_j}, \tag{13}$$

where Z_i is the height of the suspension column at time t_i, $t_0 = 0$, $z_0 = L_j$, L_j is the initial height of the column at j-th

test and N_j is the number of measurements made during the j-th test. The first part of a data set obtained during one of the batch tests is depicted by square marks in Fig. 3. If we denote $Y(t)$ the height of the lower interface above the bottom at time t, i.e. the level below which $c > c_0$, the zone between the interfaces contains suspension at the initial concentration c_0:

$$c(x,t) = c_0 \text{ for } t > 0 \quad \text{and} \quad x \in (Y(t), Z(t)), \tag{14}$$

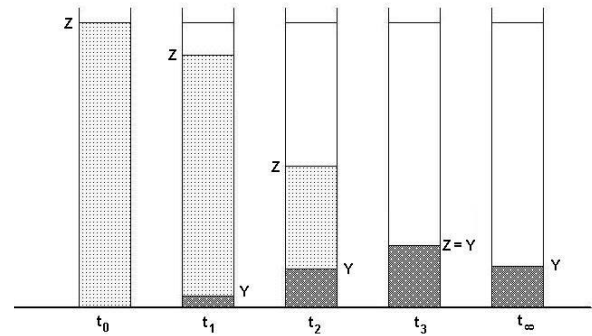see Fig. 2. We will utilize this knowledge when solving the following forward problem.

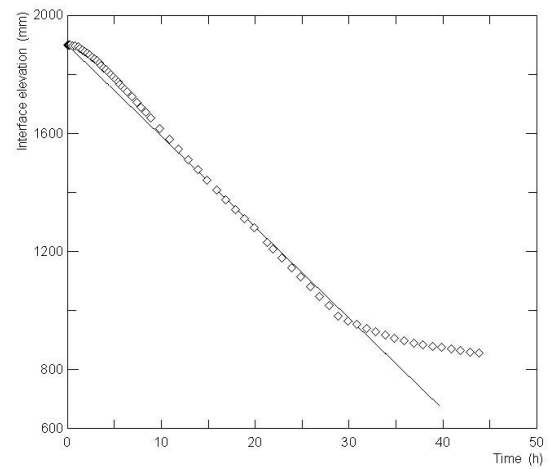**Fig. 2.** Development of the suspension profile during the experiments.

Fig. 3. Test No. 7 – function $Z(\mathbf{t})$ and the measured values.

A FORWARD PROBLEM AND ITS SOLUTION

Let us suppose that there is a region below the upper interface where there is the constant concentration c_0 of the suspension for certain time interval. In virtue of continuity Eq. (1), the volumetric flux density of the liquid phase does not depend on the space coordinate x and is a function of time only. Hence, the Eq. of motion (9) becomes the following ordinary differential equation

$$\frac{\partial w}{\partial t} + \frac{g\rho_w n_0}{(1-n_0)K(c_0)(\rho_w + n_0(\rho_s - \rho_w))} w =$$
$$= \frac{g(\rho_s - \rho_w)n_0(1-n_0)}{\rho_w + n_0(\rho_s - \rho_w)}, \tag{15}$$

where n_0 is the initial value of porosity related to the initial concentration c_0 by Eq. (10). According to conditions (12), the initial condition is

$$w(0) = 0. \tag{16}$$

The solution to the problem (15), (16) is the function

$$w(t) = \rho(1-n_0)^2 K(c_0)$$
$$\left(1 - \exp\left(\frac{-gn_0 t}{(1-n_0)(1+\rho n_0)K(c_0)}\right)\right), \tag{17}$$

where

$$\rho = \frac{\rho_s - \rho_w}{\rho_w} .$$

Denote by v_s the speed of solid-phase particles. Then, according to the definition of the volumetric solid-phase flux density, it holds

$$v = (1-n)v_s$$

and at the same time

$$v_s = \frac{dZ}{dt} ,$$

as the upper interface moves down with the solid-phase particles. The last two equations together with relations (8) and (17) enable us to formulate the following ordinary differential equation for the height of the upper interface

$$(1-n_0)\frac{dZ}{dt} = -\rho(1-n_0)^2 K(c_0)$$
$$\left(1 - \exp\left(\frac{-gn_0 t}{(1-n_0)(1+\rho n_0)K(c_0)}\right)\right) \tag{18}$$

supplemented with the initial condition

$$Z(0) = L , \tag{19}$$

where L is the initial height of the suspension column. Then, the solution to the last problem is

$$Z(t) = L - \rho(1-n_0)K(c_0)t + \frac{\rho(1+\rho n_0)(1-n_0)^2 K(c_0)}{gn_0}^2$$
$$\left(1 - \exp\left(\frac{-gn_0 t}{(1-n_0)(1+\rho n_0)K(c_0)}\right)\right). \tag{20}$$

Function Z given by Eq. (20) satisfies every one of the 45 data sets (13) provided all the parameters L, ρ, n_0 and $K(c_0)$ agree with the parameters of the test and $t \in (0, t_m)$, where

$$t_m = \sup\left\{\vartheta \in R^1; Z(t) > Y(t),\, t \in (0, \vartheta)\right\} .$$

Fig. 3 shows measured values of the upper interface elevation and the associated curve $Z(t)$ given by Eq. (20). Splitting of these curves is clearly visible indicating that t_m lies close to 30 hours. Also it can be seen from the figure that the derivatives of both curves decrease at the beginning until they become almost constants. While the theoretical function approaches very quickly to its asymptote, in minutes, the measured data obtain the linear form after several hours. This phenomenon was observed in all the experiments and can be explained by an initial instability of the suspension column.

DETERMINATION OF THE FUNCTION $K(c)$

Every one of the 45 tests started with its own parameters L, ρ, n_0 and $K(c_0)$. The only unknowns among them were the values $K(c_0)$. The remaining values L, ρ, and n_0 are measurable and were determined. To get the values $K(c_0)$, the sum $S(K)$ of squares of differences between the theoretical function Z and measured data (t_i, z_i),

$$S(K) = \sum_{i=1}^{N} (z_i - Z(t_i))^2, \tag{21}$$

was minimized, where the integer N satisfied the condition $t_N < t_m$. The problem leads to a nonlinear equation of a third-order polynomial in the unknown $K(c_0)$ containing moreover an exponential term. Let us denote

$$\zeta_i = L - z_i ,\ A = \rho(1-n_0) ,$$

$$B = \frac{(1-n_0)^2(1+\rho n_0)\rho}{gn_0} ,$$

$$e_i = \exp\frac{-gn_0 t_i}{(1-n_0)(1+\rho n_0)K(c_0)} ,$$

i.e.

$$e_i = \exp\frac{-At_i}{BK(c_0)} . \tag{22}$$

The sum of squares of differences (21) is now

$$S = \sum_{i=1}^{N}\left(\zeta_i - AK(c_0)t_i + B(K(c_0))^2(1-e_i)\right)^2 . \tag{23}$$

Hence, the sum S is minimized at $K(c_0)$ satisfying equation

$$2B^2\sum_{i=1}^{N}(1-e_i)^2(K(c_0))^3 - AB\left(\sum_{i=1}^{N}e_i t_i(1-e_i) + 3\sum_{i=1}^{N}t_i(1-e_i)\right)(K(c_0))^2 + \left(A^2\sum_{i=1}^{N}t_i^2(1+e_i) + 2B\sum_{i=1}^{N}\zeta_i(1-e_i)\right)K(c_0) - A\sum_{i=1}^{N}t_i\zeta_i(1+e_i) = 0. \tag{24}$$

As the function

$$e(t) = \exp \frac{-At}{BK(c_0)}$$

converges to zero exponentially with time, the function $Z(t)$ quickly approaches its asymptote

$$\phi(t) = L - \rho(1 - n_0)K(c_0)t +$$
$$+ \frac{(1 - n_0)^2(1 + \rho n_0)\rho(K(c_0))^2}{g n_0}.$$

Hence, we are looking for such a solution of Eq. (24) that is close to the solution of the equation

$$2B^2 \sum_{i=1}^{N}(K(c_0))^3 - 3AB \sum_{i=1}^{N} t_i(K(c_0))^2 +$$
$$+ \left(A^2 \sum_{i=1}^{N} t_i^2 + 2B \sum_{i=1}^{N} \zeta_i \right) K(c_0) - A \sum_{i=1}^{N} t_i \zeta_i = 0. \quad (25)$$

It can be shown that for each data set (13) obtained from the 45 experiments, Eq. (25) has exactly one positive root κ and that Eq. (24) has exactly one root $K(c_0)$ in the interval $(\kappa / 2, 2\kappa)$. According to this knowledge, the 45 unknown values $K(c_0)$ were found by the interval bisection method. Fig. 3 shows the data (t_i, z_i) obtained from one of the batch tests and the function $Z(t)$ with the corresponding solution $K(c_0)$. The splitting of the depicted functions, which is clearly visible in the figure, indicates the time t_m at which $Z(t_m) = Y(t_m)$ and both the interfaces meet. It is also evident that, when looking for $K(c_0)$, only those elements (t_i, z_i) of the set (13) can be utilized that satisfy the condition $t_i < t_m$. It was found that the starting value κ is very close to the solution $K(c_0)$, i.e. that the linear function

$$\varsigma(t) = L - \rho(1 - n_0)\kappa t + \frac{(1 - n_0)^2(1 + \rho n_0)\rho\kappa^2}{g n_0}$$

fits the measured data almost as well as the function (20).

Connecting the obtained values $\left(K(c_0) \right)_i$, $i = 1,...,45$ with the starting conditions of the i-th test, particularly with values $(c_0)_i$, a new data set was obtained:

$$\left\{ c_i, K_i \right\}_{i=1}^{45}, \quad (26)$$

where the notation was simplified writing c_i and K_i instead of $(c_0)_i$ and $\left(K(c_0) \right)_i$, respectively. Analyzing the data (26) it was realized that the hydraulic conductivity decreases with concentration in the whole region and that the nature of the decrease is of a power form for lower values of concentration and exponential for its higher values. Using again the least squares method for logarithms of hydraulic conductivity and requiring moreo-ver certain degree of smoothness, the unknown function $K(c)$ was determined. Particularly the sum

$$S = \sum_{i=1}^{45} \left(\ln(K_i) - \ln((K(c_i)) \right)^2,$$

was minimized, and $K \in C^1(D)$ was required, where D is the domain of the function K. Eventually, the following results were achieved:

$$D = [4.50, 421],$$
$$K = A_1 \times c^{B_1} \text{ for } c \in \left[4.50, 95.7438 \right],$$

$$K = A_2 \times B_2^c \text{ for } c \in \left[95.7438, 421 \right],$$

where

$$A_1 = 0.44872, \ B_1 = -1.8578,$$
$$A_2 = 6.0028 \times 10^{-4}, \ B_2 = 0.98078. \quad (28)$$

Figs 4 and 5 show the curve $K(c)$ in two different scales; the solid curves depict the obtained function $K(c)$ and the points (the squares) are the values of K computed from the 45 batch tests using the above described method. The bold line shows the power function and the thin line shows the exponential function. The different scales of the c-axes in the figures were chosen in order to make visible how the function changes its nature. The vertical dashed lines in the figures denote the precise position of the threshold of separation.
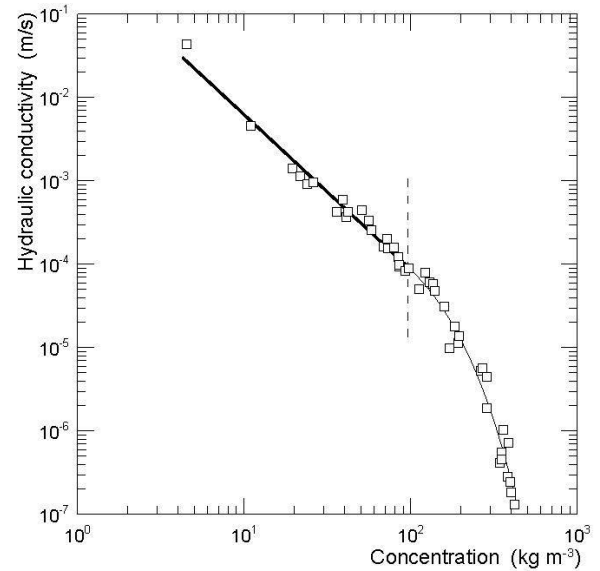

Fig. 4. Function $K(c)$.

CONCLUSIONS

The hydraulic conductivity of water and kaolin suspension as a function of its concentration was investigated. Instead of measuring the hydraulic conductivity directly, 45 batch tests were carried out and, during each of them, couples of time and height of the suspension column were measured. Making use of Darcian mechanics of two-phase systems, Eq. (1) to (4), it was

possible to find the solution (20) of the direct problem. The solution of the corresponding inverse problem is based on the comparison of the solution (20) with the measured data. As the solution describes the settling process in its initial phase, before the zone of compression reaches the top of the suspension column, the obtained value of hydraulic conductivity corresponds to the initial concentration of the measured test.
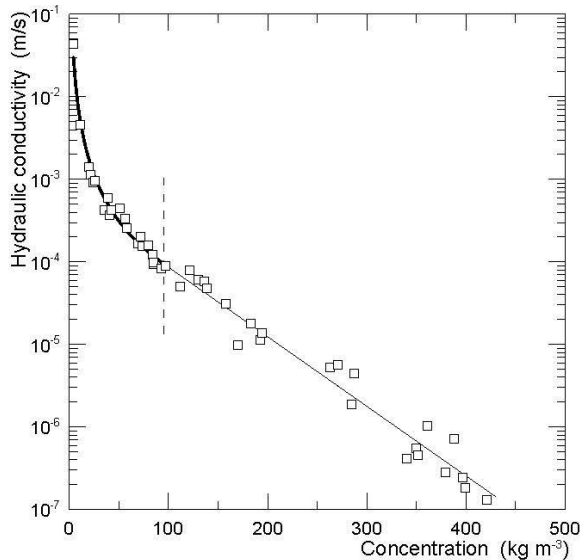

Fig. 5. Function $K(c)$.

The hydraulic properties of a suspension strongly depend on its degree of coagulation. To achieve uniqueness of obtained results, the coagulation was precisely defined for every concentration as the rate of added Calcium(II) chloride and the mass of the solid phase. Particularly 4 g of $CaCl_2$ were added to 1 kg of the solid phase. In this way, the material is considered as different concentrations of one suspension.

Analysis of the results made it possible to determine the dependence of hydraulic conductivity on the suspension concentration i.e. the function $K(c)$. Denoting the domain of measured concentrations D, the requirement $K \in C^1(D)$ has been satisfied. Moreover, it was find that the dependence changes its nature. A point ξ was determined such that $\xi \in D$ and, as the concentration increases, the function K changes at ξ from a power function to an exponential function.

REFERENCES

Coe, H.S., Clevenger, G.H., 1916. Methods for determining the capacity of slime-settling Tanks. AIME Trans., 55, 356–384.

Kynch, G.J., 1952. A Theory of Sedimentation. Transactions of the Faraday Society, 48, 166–176.

Landman, K.A., White, L.R., Buscall, R., 1988. The continuous flow gravity thickeners: steady state behaviour. AIChE, 34, 239–252.

Mls, J., 1995. Determination of Hydromechanical Characteristics of a Suspension. In: Wrobel, L.C., Šarler, B., Brebbia, C.A., (Eds): Computational Modelling of Free and Moving Boundary Problems III. Computational Mechanics Publications, Southampton, Boston.

Mls, J., 1999. A continuum approach to two-phase porous media. Transp. in Porous Media, 35, 15–36.

Mls, J., 2005. A Contribution to the Problem of the Continuous Dewatering Process. In: Mammoli, A.A., Brebbia, C.A., (Eds): Computational Methods in Multiphase Flow III. WIT Press, Southampton, Boston.

Mls, J., Herrmann, L., 2011. Oscillations for an equation arising in groundwater flow with relaxation time. Mat. Model. and Anal., 16, 4, 527–536.

Nasser, M.S., James, A.E., 2007. Numerical simulation of the continuous thickening of flocculated kaolinite suspensions. Int. J. Miner. Process., 84, 144–156.

Šatava, V., 1973. Theory of ceramic casting-slips liquefaction and optimization of the casting Process. Sklář a keramik, 23, 195–199. (In Czech.)

Usher, S.P., Scales, P.J., 2005. Steady state thickener modelling from the compressive yield stress and hindered settling function. Chem. Engng J., 111, 253–261.

Van Olphen, H., 1963. An Introduction to Clay Colloid Chemistry. Interscience, New York.

Vlasak, P., Kysela, B., Chara, Z., 2012, Flow structure of coarse-grained slurry in a horizontal Pipe. J. Hydrol. Hydromech., 60, 2, 115–124.